The Susceptibility of Pure Tubulin to High Magnetic Fields: A Magnetic Birefringence and X-Ray Fiber Diffraction Study

W. Bras,*# G. P. Diakun,# J. F. Díaz,¶ G. Maret,§ H. Kramer,§ J. Bordas,# and F. J. Medrano#
*AMOLF Kruislaan 407, 1098 SJ, Amsterdam, Netherlands; #CCLRC Daresbury Laboratory, Warrington WA4 4AD, England; §High Magnetic Field Laboratory, Grenoble, France; and ¶KU Leuven, Laboratory for Chemical and Biological Dynamics, Leuven, Belgium

ABSTRACT The orientational behavior of microtubules assembled in strong magnetic fields has been studied. It is shown that when microtubules are assembled in a magnetic field, they align with their long axis parallel to the magnetic field. The effect of several parameters known to affect the microtubule assembly are investigated with respect to their effect on the final degree of alignment. Aligned samples of hydrated microtubules suitable for low-resolution x-ray fiber diffraction experiments have been produced, and the results obtained from the fiber diffraction experiments have been compared with the magnetic birefringence experiments. Comparisons with earlier fiber diffraction work and small-angle x-ray solution scattering experiments have been made.

INTRODUCTION

One of the more difficult problems in the preparation of biological samples suitable for high-resolution x-ray fiber diffraction is the exact alignment of the molecules. In some exceptional cases, spontaneous orientation of a concentrated gel can be utilized (Bernal and Fankuchen, 1941). However, in general, other techniques have to be used. For instance, orientation can be induced by shearing (Popp et al., 1987), centrifugation (Mandelkow et al., 1977), pulsed electric fields (Koch et al., 1995), and static magnetic fields (Torbet, 1987). The latter method is the least invasive, as it relies on the interaction of the small diamagnetic moment of suitable molecules with strong magnetic fields. This has become possible with the advances made in superconducting magnet technology, which have made available fields of up to ~15 T, even outside the specialized high magnetic field laboratories (Maret and Dransfeld, 1985).

If a molecule (without an unpaired electron) is placed in a uniform magnetic field, the intramolecular screening currents generate a diamagnetic moment, μ, proportional to the magnetic field H:

$$|\mu| = \chi|H| \tag{1}$$

The diamagnetic susceptibility, χ, of a molecule is closely related to its structure and is therefore generally anisotropic. This diamagnetic anisotropy leads to an orientation of the molecule in the magnetic field. Examples are aromatic amino acids, where nonlocal ring currents are generated, resulting in a large diamagnetic anisotropy, or nonaromatic molecules without nonlocal ring currents, the diamagnetic anisotropy of which is given, to a first approximation, by the sum of the local anisotropies of the interatomic bonds (Maret and Dransfeld, 1985). The peptide bond has a partial double-bond character at resonance and is therefore thought to exhibit diamagnetic anisotropy, although different magnitudes of the diamagnetism have been reported (Worcester, 1978; Pauling, 1979). It is noteworthy that when amino acids are arranged in an α-helix, peptide bonds are all lying in a plane parallel to the helical axis. Assuming the helix to be a rigid structure, the total susceptibility is determined by the vectorial addition of the individual susceptibilities along the principal axes, thus rendering a much higher value. Successful orientation of several α-helical structures by magnetic fields has been reported, notably by Samulski and Tobolski (1971), who managed to align poly(gamma-benzyl L-glutamate), a highly α-helical structure, in a magnetic field of moderate strength.

Several alignment methods have been reported that are completely based on the use of magnetic fields or on magnetic fields combined with other techniques. Notable examples are solutions of virus molecules in a magnetic field from which the water is evaporated (Torbet and Maret, 1979; Nave et al., 1981), so that the aligning action of the field is supported by the occurrence of steric hindering effects. This method, however, has the drawback that the hydration of the samples is changed, which can possibly lead to denaturation of the protein or conformational changes. Polymers formed by the addition of monomers to oligomers in the presence of a strong magnetic field (Torbet and Ronzière, 1984) have also shown a high degree of alignment. This method has the clear advantage that it does not alter the biochemical state of the protein, i.e., no degradation or conformational changes are likely to occur.

Microtubules, macromolecules that are a common part of the cytoplasm of all eukaryotic cells, are a suitable candi-

Received for publication 25 November 1996 and in final form 8 December 1997.

Address reprint requests to Dr. Wim Bras, Dubble CRG/ESRF, BP 220, F-38043 Grenoble Cedex, France. Tel.: +33-(0)4-76882351; Fax: +33-(0)4-76882412; E-mail: bras@esrf.fr.

Dr. Medrano's present address is Max Planck Intitute of Biochemistry, Abtl. Huber, Am Klopferspitz 18 AD, 82152 Martinsried, Germany.

Dr. Maret's present address is Institut Charles Sadron, 6, rue Boussingault, Strasbourg, France.

Dr. Bordas's present address is Department of Physics, Liverpool University, P.O. Box 147, L69 3BX Liverpool, England.

0006-3495/98/03/1509/13 $2.00

date for alignment in a magnetic field, using the method of assembly in the magnetic field. They are large macromolecular assemblies composed of elongated protofilaments (Hyams, 1979). The protofilaments are formed by connecting tubulin heterodimers (kidney-shaped molecules consisting of nearly identical α- and β-monomers) in a head-to-tail fashion. The protofilaments are connected laterally to form a thick-walled cylinder, and the number of protofilaments involved in this process ranges between 11 and 17, but with the biochemical conditions that we have employed the predominant number is 13 (Andreu et al., 1992).

Closely associated with the microtubules is a group of proteins called microtubule-associated proteins (MAPs), which interact with the microtubules and protrude from the microtubule wall up to a distance of ~90 nm (Hirokawa et al., 1988). Under the appropriate biochemical conditions, microtubules can be assembled from tubulin heterodimers by raising the temperature from 4°C to 37°C (Bordas et al., 1983; Lee and Timasheff, 1977). When the microtubules have formed, they cannot be seen as static macromolecules, but are in a dynamic equilibrium with the pool of free tubulin dimers in the solution (Rothwell et al., 1986). This can be termed *treadmilling,* where the microtubule is growing at one end and shrinking at the other. The microtubule assembly process can be described by the following reaction equation:

$$\mathrm{MT}(n-1) + \mathrm{TbGTP} \overset{K_c}{\rightleftarrows} \mathrm{MT}(n) \qquad (2)$$

in which MT(n) represents a microtubule with n dimers, TbGTP a dimer with the necessary GTP, and K_c the association constant for the binding of one dimer to the microtubule, which is the inverse of the critical concentration value below which no assembly will take place.

The assembly of microtubules is induced in vivo by the presence of MAPs, which also promote in vitro assembly of tubulin. For some time it was thought that they were necessary for this assembly. This is not the case, inasmuch as it was shown that the purified tubulin contains all of the information needed to produce microtubules, although the critical concentration is raised. Nevertheless, this critical concentration can be reduced to acceptable values in the presence of specific promoters of polymerization like glycerol or dimethyl sulfoxide (Lee and Timasheff, 1977). A consequence of assembly without MAPs is that, depending on the protein concentration, a fraction of 5–10% remains unassembled. Further details on the assembly process are extensively discussed in the literature, but are beyond the scope of this paper (Himes et al., 1977; Andreu et al., 1989; Diaz et al., 1996).

An indication that magnetic fields are indeed suitable for aligning microtubules can be found in Amos (1979), where it is stated that there is some evidence that tubulin dimers have a relatively high proportion of α-helices oriented along their long axis. Circular dichroism experiments indicate that ~25% of the amino acids have an α-helical structure (Lee et al., 1978; Ventilla et al., 1972). This implies that the assembled microtubules may exhibit a relatively strong diamagnetism, because the direction of the dimer axis coincides with the direction of the axis of the assembled macromolecule. The vectorial addition of the diamagnetic anisotropies can render a resultant magnetic anisotropy that is orders of magnitude larger than that from the single dimer. In addition to the contribution of α-helices, a possible contribution of aromatic amino acids, which in tubulin make up ~10% of the total number of amino acids, could be added to this. Because the diamagnetic anisotropy of individual aromatic amino acids is much stronger than that of most other molecular groups, it is possible that they dominate any alignment of the microtubules in a magnetic field.

A susceptibility to magnetic fields of isolated microtubules has been reported by Vassilev et al. (1982), who claim to have observed alignment, in modest magnetic fields of up to 0.02 T, such that the long axis of the molecule coincided with the magnetic field direction. From magnetic birefringence experiments it is known that bulk samples are known to show some degree of alignment, but no attempts have been made to quantify these (Torbet, 1995). Mandelkow (1986) claimed that cross-linking between the molecules will inhibit alignment in magnetic fields, but as we will show, this is not necessarily the case if the molecules are in the aligned state before cross-linking can take place or if the cross-linking can be inhibited.

To our knowledge, conventional techniques for sample alignment (e.g., shearing) have not produced hydrated microtubule samples with sufficiently high degrees of (uniform) alignment (Hitt et al., 1990) to be able to perform quantitative fiber diffraction experiments. The most successful fiber diffraction results on partially hydrated microtubule protein so far have been obtained with an alignment method developed by Mandelkow et al. (1977) or by using naturally occurring fibers in giant axons (Wais-Steider et al., 1987). In the first case, the protein was centrifuged for an extended period (24 h) to obtain a sample with a protein concentration over 30 mg/ml and a high degree of alignment. However, the rigorous sample preparation method is likely to have consequences for the structure of the molecule, which might be forced into a semicrystalline state and possibly undergo a conformational change in the process (Nave et al., 1979), and the degree of hydration. The diffraction results obtained from the giant axon fibers are in reasonable agreement with the work of Mandelkow et al. (1977). However, the low-resolution intensity distribution on the equator of the fiber diffraction pattern decays more slowly when compared to the intensity decay observed in solution scattering experiments (Andreu et al., 1992). A possible explanation for this could be that the microtubules in the centrifuged and fiber samples are in close proximity and thus interact with each other, either directly via surface charges or indirectly via the MAPs. It is possible that a degree of crystallographic packing will develop as a result of this interaction. This in itself would generate another diffraction pattern, so that in a diffraction experiment one

would not measure the molecular transform of the microtubule, but the molecular transform sampled on reciprocal lattice points of the crystallographic register. Therefore we have investigated the possibility of using a less intrusive method of sample alignment, so that the likelihood of any conformational changes would be minimized, and problems associated with the regular packing in a fiber could be avoided. To this end, we have employed high magnetic fields to align microtubules and have determined the degree of alignment by using x-ray fiber diffraction. We have also studied the dynamics of microtubule assembly and alignment by magnetic birefringence.

It can be remarked that if it would be possible to use the method of magnetic alignment to obtain a very regular packing and a very high degree of orientation, this in itself would be an extremely interesting result and would allow conventional methods of protein crystallography to be used to make possible high-resolution structural studies of assembled microtubules that could be complementary to research on the structure of tubulin dimers (e.g., Nogales et al., 1995).

THEORETICAL CONSIDERATIONS

To correctly determine the diamagnetic moment of an assembled microtubule, all of the contributions of the separate components have to be added. For this the accurate angular positions of the components have to be known. This would require detailed knowledge of the structure of the tubulin dimer. Because of the lack of crystallographic studies at sufficiently high resolution, this is not feasible, and therefore we have tried with a simplified model to gain insights into the minimum field necessary to obtain an orientation effect on an assembled microtubule. The possibility cannot be excluded that the orientation of a single dimer in a magnetic field is different and will not be parallel to the magnetic field, as is the assembled microtubule. The latter is the case, as we have found empirically.

For an order-of-magnitude calculation on the strength of the magnetic field necessary for the successful alignment of pure microtubules in solution (i.e., without the influence of MAPs), we have to estimate the minimum strength of the diamagnetic anisotropy first. The average number of dimers in a microtubule can be determined by using data on the average microtubule length (Pirollet et al., 1987; Diaz, unpublished observations). Pirollet estimates that after reaching equilibrium, 90% of the microtubules have a length between 0 and 10 μm. Assuming that the average length will be 5 μm, the dimer length to be 8 nm, and the average number of protofilaments composing the microtubule wall to be 13, an estimate of the average number of dimers in a microtubule, N_d, can be calculated to be ~8125. Experiments on the flexural rigidity of microtubules indicate that the microtubules can be considered to be rigid rods. Gittes et al. (1993) have determined a value of 5200 μm for the persistence length. Venier et al. (1994) have determined a value of 2000 μm. Both values exceed the average value determined by Pirollet et al. (1987) by roughly three orders of magnitude. The cylindrical symmetry of the assembled microtubules allows us to simplify the problem. When we decompose the forces on the individual dimers in a component parallel and perpendicular to the long microtubule axis and assume that the microtubules will align parallel to the magnetic field, it can be assumed that the perpendicular components of the force on the opposing parts of the cylinder wall will compensate each other. This allows us to consider only the components of the diamagnetic anisotropies of the dimers that are parallel to the main (long) microtubule axis, $\Delta\chi_d$, to obtain an estimate of the minimum average aligning force on the molecule. This value is as yet an unknown, but a minimum value can be estimated if it is assumed that the diamagnetism is due entirely to α-helices aligned parallel to the dimer axis:

$$\begin{aligned}\Delta\chi_{total} &= N_d \times \Delta\chi_d \\ &= N_d \times N_p \times f_1 \times f_2 \times \frac{\Delta\chi_p}{N_a} \times C \\ &= 8125 \times 888 \times 0.25 \times 0.5 \times \frac{5.36 \times 10^{-6}}{6.02 \times 10^{23}} \times 4\pi \\ &\quad \times 10^{-6} \\ &\approx 1.01 \times 10^{-28}[\mathrm{m}^3] \end{aligned} \quad (3)$$

where N_d is the number of dimers in a microtubule (± 10% error margin); N_p is the estimated number of peptide bonds in dimer (± 2%) (Little and Seehaus, 1988); f_1 is the estimated fraction of peptides in α-helices (± 20%); f_2 is the estimated fraction of peptides in α-helices along dimer axis (± 20%); $\Delta\chi_p$ is the anisotropy of the molar susceptibility of the peptide bond (Pauling, 1979) (± 5%); $\Delta\chi_d$ is the anisotropy of the magnetic susceptibility of the tubulin heterodimer; N_a is Avogadro's number; C is a conversion factor. (The conversion factor is essential for obtaining the value in SI units. It is composed of a factor 4π from the conversion of the $\Delta\chi$ value and a factor 10^{-6} from the conversion from cm^3 to m^3.)

With the error margins indicated, the probable error in this number will be on the order of 25%.

This value is probably too low, because it ignores the possible contribution to the anisotropy of aromatic amino acids whose anisotropy is roughly a factor 10 stronger than that of a single peptide bond. As remarked by Maret and Dransfeld (1985), the aromatic amino acids might contribute considerably to the diamagnetic anisotropy when coupled in their orientation to a polypeptide chain. In the case where the plane of an aromatic amino acid is fixed at a right angle with respect to the microtubule axis, this would generate a tendency to align at right angles with respect to the applied magnetic field. Because of the nearly cylindrical symmetry, forces generated on aromatic rings with a fixed angular position other than 0° or 90° on opposing parts of

the microtubule wall will tend to compensate each other. As will be shown later in the text, the microtubules align parallel with respect to the applied magnetic field, in agreement with the findings of Vassilev et al. (1982). The value of f_2 is probably overestimated, but in this order-of-magnitude calculation it can be used to take into account the effect of partially aligned α-helices and β-sheets.

Ignoring the effects of aromatic amino acids for the time being, an estimate of the minimum magnetic field strength needed for alignment can be made. A necessary condition is that the magnetic energy is at least comparable to the thermal energy of the molecule:

$$\frac{\Delta\chi_{\text{total}}B^2}{2\mu_0} \geq \frac{kT}{2} \tag{4}$$

This leads to

$$B \geq \left(\frac{\mu_0 kT}{\Delta\chi_{\text{total}}}\right)^{1/2} = \left(\frac{4\pi \times 10^{-7} \times 1.38 \times 10^{-23} \times 300}{1.01 \times 10^{-28}}\right)^{1/2}$$

$$\approx 7.6 \text{ Tesla} \tag{5}$$

The error margin in $\Delta\chi_{\text{total}}$ we have estimated above to be 25%, and assuming kT to be exact, we come to an error margin of ~15% of this number. This order-of-magnitude calculation indicates that one does not have to use unrealistically high fields to obtain some alignment. These figures are supported by calculations made by Torbet (1987), who claims that to align 80% of a molecule in a 10-T field, 1.5×10^7 peptide bonds are needed.

Possible effects that might counteract the alignment are cross-linking, the repulsive effect of surface charges on the molecule, aromatic amino acids with their planes at right angles to the microtubule axis, and steric hindering. Furthermore, a mechanism of spontaneous alignment observed by Pirollet et al. (1987) might have a negative effect when the orientation vectors for the spontaneous and magnetically induced orientation do not coincide. From these effects, the cross-linking can be avoided by using pure tubulin without the MAPs. The latter are thought to be initiators of cross-linking (Wicke, 1985). Orientational effects due to structural correlations between ordered components of the buffer solution and the microtubules are deemed to be of minor importance, because the largest molecule in the buffer solution is glycerol, with a negligible magnetic moment (Sosnick et al., 1991; Hayter et al., 1989).

It is known, both from theory (Onsager, 1949; Vroege and Lekkerkerker, 1992) as well as experiment (Bernal and Fankuchen, 1941), that solutions of rigid rods can spontaneously phase separate in an isotropic and a nonisotropic phase. This effect is concentration-dependent. For the microtubule concentrations used in this work, we can assume the dilute regime according to the definitions of Edwards (1966). In the more specific case, when one is considering the possibility of liquid crystal formation in rigid rod solutions, the important parameter is the excluded volume, as discussed by Vroege and Lekkerkerker (1992). These authors show that phase separation can be expected when the concentration is such that the available volume for a single macromolecule approximates the excluded volume, whereby the excluded volumes scales with l^2d (l = length, d = diameter of the macromolecule). For the concentration used in this work, the available volume per macromolecule is between 5 and 10 times as large as the excluded volume.

The previous discussion deals only with a situation in which we are considering molecules of a fixed length (or fixed length distribution) without external forces. For most of the experiments described in this work, these assumptions are valid in the final state. However, for microtubules assembled in a magnetic field, we have used a slightly different approach to assess steric hindering effects. An order-of-magnitude calculation on the onset of steric hindering of alignment can be made. The assumption is made that a molecule becomes restricted in its movements when a second molecule is inside a sphere with its origin at the center of gravity of the molecule and a radius half the length of the molecule. When the total volume defined in this way exceeds the total available volume, one can expect the onset of steric hindering. For calculation purposes, the assumption is made that the microtubule grows in rings of 13 laterally connected dimers. The second assumption is that all microtubules grow at a similar rate, so that the volume per molecule is simply a function of the length of the molecule. The total number of dimers (N_{dim}) in a given volume (in this calculation 10^{-6} m^3) can be calculated from the protein concentration. If, for example, a concentration of 4 mg/ml is used, we calculate that $N_{\text{dim}} \approx 2.19 \times 10^{16}$. In Fig. 1 the results are shown for a solution with a protein concentration of 4 mg/ml.

In this example the excluded volume exceeds the real available volume when the molecule length is ~50 times the length of a single dimer. A variation in the concentration (i.e., N_{dim}) shifts the curve horizontally. Thus theoretically the alignment will be either total or completely absent,

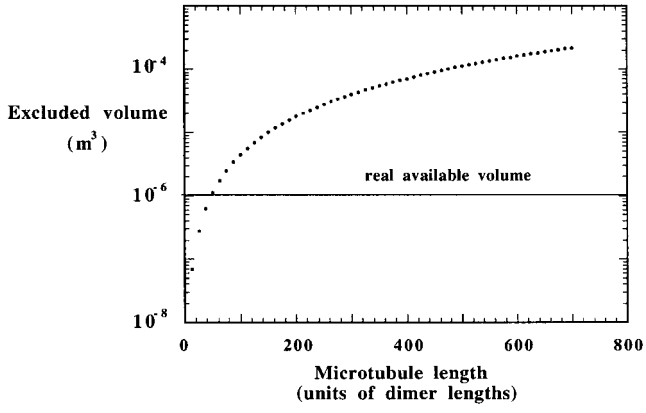

FIGURE 1 Total volume occupied by spheres with a radius of half the microtubule length, as a function of the microtubule length expressed in number of dimers. Protein concentration: 4 mg/ml. As soon as the volume exceeds the total available volume, steric hindering effects can be expected.

depending on the initial orientation of the dimer, when the concentration is at the level that the available volume will be exceeded when the molecule length is on the order of the diameter of the molecule. On the basis of these coarse calculations, this limit is ~65 mg/ml. From these considerations, we also conclude that it is essential that the magnetic field be applied from the onset of assembly. The importance of this decreases at later stages, because once aligned, the microtubules will be inhibited to rotate away from the axis of preferred orientation because of steric hindering. Clearly, this does not take account of the possible perturbing effects that intermediate assembly states in the assembly pathway may have, such as a different conformation (Nogales de la Morena, 1992), and consequently the effects a different diamagnetic anisotropy from the fully assembled molecule might have.

Another important parameter to be considered in fiber diffraction experiments is the distance between aligned microtubules. If the microtubules are too close, a possible (liquid) crystalline packing of the microtubules might occur. As an approximation, a calculation was made of the intermicrotubule distance in the case where the molecules were placed on a hypothetical cubic lattice (see Fig. 2). Furthermore, a concentration-dependent intrinsic misalignment angle was determined based on the diameter of a cylinder of the average microtubule length and the average intermicrotubule distance. The misalignment angle is defined as the angle that a linear chord of maximum length can make with the cylinder axis.

From Fig. 2 it can be seen that the intermicrotubule distance, d, for a protein concentration below 10 mg/ml is 120 nm. In a diffraction pattern this will translate to a possible first diffraction maximum due to the crystalline packing at $s = 8.3 \times 10^{-3}$ nm^{-1} ($s = 1/d$ nm^{-1}). The first strong diffraction peak due to the molecular transform will be located at $\sim 4.3 \times 10^{-2}$ nm^{-1}. Taking into account the intrinsic misalignment angles, it can be assumed that no diffraction intensity due to the crystallographic packing will be observed in the diffraction region of interest.

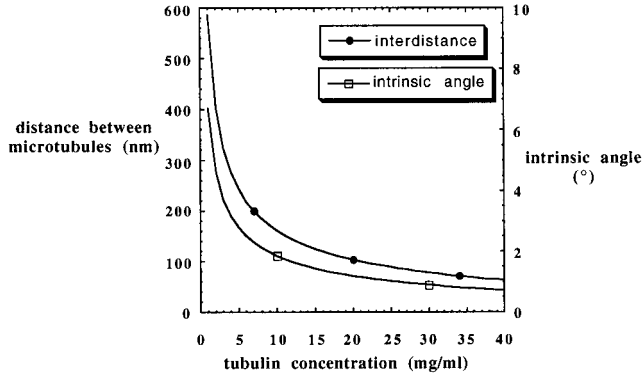

FIGURE 2 The pure intermicrotubule distance as a function of the protein concentration (*left-hand scale*). Also shown is the intrinsic misalignment angle (*left-hand scale*), which is defined as the maximum angle that a chord inside the free available volume described by a cylinder around the microtubule with a radius equal to the intermicrotubule distance can make with the axis of this cylinder. This value is an estimate of the minimum angular spread in an oriented microtubule solution.

In birefringence experiments, the optical anisotropy of a sample plays an important role. This has an unknown value for tubulin dimers, but an order-of-magnitude calculation can (indirectly) be made. We make use of the well-known fact that optical anisotropy, $\Delta\alpha_0$, and diamagnetic anisotropy, $\Delta\chi$, are correlated (Torbet and Maret, 1981) to estimate the optical anisotropy of a single peptide bond. The diamagnetic anisotropy of a peptide bond is approximately two-thirds of that of the C═C bond (Maret and Dransfeld, 1985), and we assume that the same relation holds for the optical anisotropy. The optical anisotropy for a C═C bond is 3×10^{-30} m^3 (Mills, 1972). Therefore we use the value $\Delta\alpha_0 = 2 \times 10^{-30}$ m^3 for the peptide bond. If we then use the same assumptions concerning the number of peptide bonds in α-helices parallel to the dimer axis as outlined in Eq. 2, we calculate a total optical anisotropy for a microtubule of average length, $\Delta\alpha_{0,\text{total}}$, to be 2.26×10^{-34} Fm^2. This can be correlated to the saturation birefringence by

$$\Delta n_{\text{sat}} = \frac{N\Delta\alpha_{0,\text{total}}}{2n\varepsilon_0} = 2.6 \times 10^{-5} \tag{6}$$

in which N is the number of microtubules per unit volume, n is the refractive index ($n = 1.33$), and $\epsilon_0 = 8.85 \times 10^{-12}$ As/Vm. For a pure microtubule solution of 4 mg/ml, the value of $N = 2.7 \times 10^{12}$. The birefringence, Δn, of a partially aligned solution is given by

$$\Delta n = \Delta n_{\text{sat}}\Phi \tag{7}$$

in which Φ is the Herman's orientation function. It has to be mentioned that the error margins are even larger than the margins estimated for the diamagnetic anisotropy, because the optical polarizability for the peptide bond was determined rather indirectly.

MATERIALS AMD METHODS

Biochemistry

Tubulin was purified from pig brain, stored in liquid nitrogen, and prepared for use as described elsewhere (Weisemberg et al., 1968; Lee et al., 1973; Andreu et al., 1989). Tubulin concentrations were determined spectrophotometrically by employing an extinction coefficient of 107,000 M^{-1} cm^{-1} at 275 nm in 10 mM phosphate buffer containing 1% sodium dodecyl sulfate (pH 7.0) (Andreu et al., 1984).

For assembly, tubulin was equilibrated in 10 mM sodium phosphate, 3.4 M glycerol, 1 mM EDTA, 0.1 mM GTP buffer (pH 7.0), and then 1 mM GTP and the desired concentration of $MgCl_2$ were added.

The samples were centrifuged for 10 min at 50,000 rpm and 4°C in a TLA 100.3 Beckman rotor, to eliminate the aggregates.

Magnetic birefringence

Magnetic birefringence experiments were performed with magnet M2 at the High Magnetic Field Laboratory in Grenoble. This is a Bitter magnet with optical access to the sample space at right angles to the applied magnetic field. The magnetic birefringence Δn was measured with a

combined photoelastic modulation and compensation technique at a wavelength $\lambda = 632.8$ nm by placing the samples in a quartz cuvette, with an internal path length of 2 mm between crossed polarizers. More details of this equipment and method can be found in Maret and Dransfeld (1985). It is not directly possible to obtain a degree of orientation from these experiments, because both the optical anisotropy as well as the intrinsic birefringence of the sample have to be determined. The birefringence values were all normalized to an arbitrary value equivalent to a protein concentration of 4 mg/ml to allow comparisons between the degrees of alignment.

Fiber diffraction

Fiber diffraction experiments were performed at the Small-Angle Diffraction stations 2.1 and 8.2 (Towns-Andrews et al., 1989; Bras et al., 1993) at the Synchrotron Radiation Source (Daresbury, England). An 11-T superconducting magnet (Oxford Instruments) was used to prepare the aligned samples. After assembly was completed, the samples were mounted on the beam line in a thermostatted sample holder (37°C). The detector and data acquisition system were described by Lewis et al. (1989).

Data reduction was carried out with the programs BSL and XOTOKO (G. R. Mant, unpublished data); the latter is the Daresbury version of OTOKO (Boulin et al., 1986). The procedure followed was essentially identical to the previously described method of Bordas et al. (1983). The degree of alignment was determined by fitting a Gaussian curve through the curve obtained after integration over a cylindrical strip containing one of the stronger diffraction peaks on the equator of the diffraction pattern. The full width at half maximum of this curve was arbitrarily defined to be the alignment degree.

It has to be remarked that the determination of the degree of alignment determined in this way is not the maximum alignment that can be achieved with a sample, because the loss of orientation when the sample is taken out of the field has to be taken into account.

Experimental protocol

In both the birefringence and the fiber diffraction experiments, the samples were first allowed to disassemble completely by lowering the temperature to 4 ± 1°C. They were equilibrated for 5 min. Subsequently the temperature was raised to 37 ± 1°C. Unless otherwise stated, the temperature ramp rate was set to 1.5°C/min. In the birefringence experiments care was taken to heat the samples as uniformly as possible to reduce the effect of temperature-induced stress on the cell walls of the quartz cuvette, which would affect the birefringence signal. Control experiments showed that the contribution of the temperature-induced stress amounted to less than 1% of the birefringence of an aligned microtubule sample with a concentration of 4 mg/ml.

The sample cells for the fiber diffraction experiments were long cuvettes with mica windows with an internal path length of 1 mm, allowing several exposures on different positions. This is essential, because during the collection of statistically significant diffraction patterns, the protein suffers from radiation damage in the intense x-ray beam. To avoid radiation damage, the diffraction patterns were collected in series of three times 1 min. Then the sample cells were translated so that the pattern from a fresh spot could be obtained. It was possible to collect up to 24 min of useful data per sample. Radiation damage became visible after ~4 min of data collection on one spot. With the help of an optical microscope equipped with cross-polarizers, we were able to establish that there was no transport of radiation-damaged material through the cell during the experiments.

To avoid confusion it should be mentioned that the birefringence results were obtained while the samples were kept in the magnetic field, whereas for the fiber diffraction experiments the samples were assembled inside the magnetic field, but after assembly was completed they were taken out of the field and were placed in the fiber diffraction camera.

RESULTS

Birefringence

An example of a result from a magnetic birefringence experiment for samples assembled in the magnetic field is presented in Fig. 3, which shows the birefringence curve for a sample that was heated from 4°C to 37°C in a magnetic field of 17.5 T.

In this figure we can distinguish several events. At 4°C the sample is completely disassembled and no birefringence is observed. Upon heating, the assembly starts and the birefringence rapidly increases, showing that the microtubules that are being formed align themselves with respect to the magnetic field axis. After maximum assembly is reached (*arrow 3*), the rate of increase of the birefringence declines but remains positive, indicating that the amount of oriented material and/or the degree of alignment increases slowly. It is unlikely that thermodynamic effects play a significant role, because of the expected entanglement of the molecules. Therefore this effect is thought to be due to the treadmilling of the microtubules. This means that disaligned samples will slowly align because of the disassembly on one side and because of the larger possibility that the free dimer will attach to an aligned microtubule due to the larger number of aligned microtubule assembly sites. A similar behavior is known from actin, which also exhibits treadmilling (Torbet and Dickens, 1984). A sample like fibrinogen, which does not treadmill, will reach a constant value of the birefringence signal (Torbet et al., 1981). When the field is switched off, a decrease in the birefringence is observed. This, however, generally stabilizes within a couple of minutes. Because the signal reached a constant value after a short decay time, it can be concluded that this is caused by microtubules that were partly mechanically forced to align with the field but, because of entanglements, settled into a

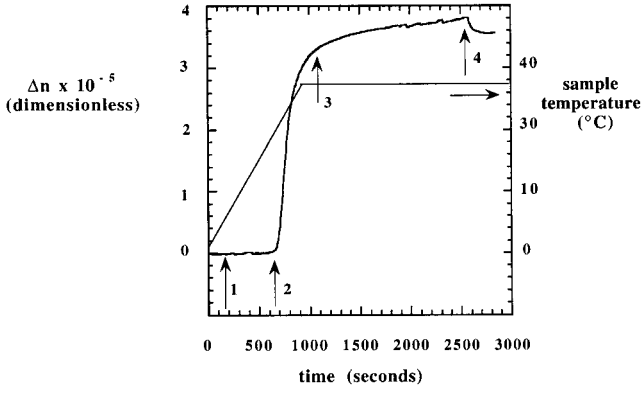

FIGURE 3 Example of birefringence signal as function of time (*left scale*). The protein concentration was 4.0 mg/ml. The solution was heated from 4° to 37°C in 20 min (*right scale*). Assembly starts around 30°C. A fast increase in the birefringence signal indicates the assembly of the protein (*arrow 2*). There is a much slower increase after assembly is complete (*arrow 3*). This increase keeps continuing over a period of more than 90 min. When the field is switched off, a slight deterioration of the alignment is observed (*arrow 4*).

lower energy state once the aligning force was taken away. On some occasions it was observed that the birefringence started to increase again once the initial loss was stabilized. This confirms the treadmilling hypothesis. The bulk of the sample remains aligned over periods in excess of 2 h. Birefringence could be observed even after 24 h outside the magnetic field in samples that were stored at room temperature. It should be remarked that it is not possible to induce tubulin assembly such a long time after sample preparation. It should be noted that the unassembled fraction of the tubulin will not contribute to the birefringence signal.

When we assume that the orientation of the molecules is nearly perfect ($\Phi = 1$) and compare the value of the birefringence, $\sim 3.8 \times 10^{-5}$, with the theoretically estimated values for the saturation birefringence, $\Delta n_{sat} = 2.6 \times 10^{-5}$ (Eqs. 6 and 7), we can conclude that there is reasonable agreement, and we can assume that the alignment of samples kept inside the magnetic field is nearly 100%. Birefringence experiments on dehydrated mitotic spindles, which are known to consist mainly of microtubules, have given birefringence values of $\Delta n = (4.4–5.0) \times 10^{-5}$ (Sato et al., 1975). Keeping in mind that these samples were dehydrated and not pure microtubules, this is in good agreement.

For the fiber diffraction experiments in which the samples are removed from the magnetic field (which is equivalent to switching off the field in the birefringence experiments), a loss of $\Delta n_{B \to 0} = 0.2 \times 10^{-5}$ was observed. If we assume that the maximum value corresponds to full alignment and that Δn is linearly related to the degree of alignment (Maret and Dransfeld, 1985), we can calculate that this loss corresponds to an angular spread of $\sim 15°$. This is very close to the angular spread determined by x-ray fiber diffraction.

A similar experiment for microtubules assembled in the presence of MAPs exhibits the same behavior but reaches a birefringence that is a factor of ~ 2 higher than the value obtained with the pure tubulin sample. This is in agreement with the experiments from Sato et al. (1975), who found that the birefringence of the mitotic spindle, consisting of microtubules and MAPs, was somewhat higher than the values found for the pure microtubules studied in this work. From fiber diffraction experiments it was found that the degree of alignment is worse than with pure microtubules. This might indicate that the MAPs have a considerable intrinsic birefringence as well.

Magnetic birefringence experiments on microtubules assembled outside the field still show a susceptibility to the magnetic field, although the signal is weaker by a factor of ~ 10 and disappears completely once the field is switched off. This effect is thought to be due to the entanglements of the molecules that will inhibit alignment, so that only strands of the microtubules will be aligned.

Attempts to measure the Cotton-Mouton constant, a measure of the value of the product of the optical and diamagnetic anisotropy (Maret and Dransfeld, 1985), for tubulin dimers were not successful because of the low signal strength.

The birefringence for a constant protein concentration was measured as a function of the applied magnetic field to determine the minimum field strength necessary to obtain the maximum achievable alignment (see Fig. 4). The samples were heated with a temperature ramp rate of 1.5°C/min inside the constant magnetic field. The protein concentration was taken to be 4 mg/ml.

These results indicate that a field of ~ 11 T is sufficient to obtain the maximum birefringence value and, consequently, the highest degree of alignment when samples with a concentration of 4 mg/ml are used. Because it is known that when (because of intermolecular interaction forces) domains are formed, there is the possibility that these domains will align better (because of the collaborative effect), the next parameter that should be considered is the effect of the protein concentration on the birefringence.

The strength of the birefringence signal has a linear dependence on the protein concentration; thus to compare the difference in alignment between the different protein concentrations, the birefringence signal has to be normalized to the concentration. Two concentration-related effects are likely to affect the alignment. The first is the excluded volume effects and consequently steric hindering effects of the elongated molecules in the assembly phase. This will have a negative effect on the final birefringence of the signal. The second effect is the possibility that liquid crystalline domains are formed that, because of the collaborative effect, will have a positive influence on the orientation. In Hitt et al. (1990) it can be found that pure microtubules indeed can exhibit nematic liquid crystalline behavior. In Fig. 5 the birefringence, normalized to a concentration of 4 mg/ml, is shown for samples of different concentration at three discrete times after onset of assembly. It is clear that a higher concentration produces a stronger birefringence signal. However, it can also be seen that the samples with the higher concentration develop the birefringence more slowly than the lower concentrations, which could indicate that domain formation plays a role.

For microtubule assembly to occur, it is generally necessary to raise the temperature above a threshold temperature

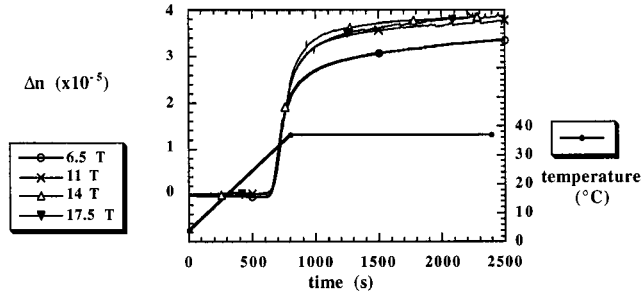

FIGURE 4 Time-resolved birefringence curves for microtubules assembled in four different constant magnetic field strengths. The assembly was initiated by raising the temperature from 4°C to 37°C at 1.5°C/min (*right scale*).

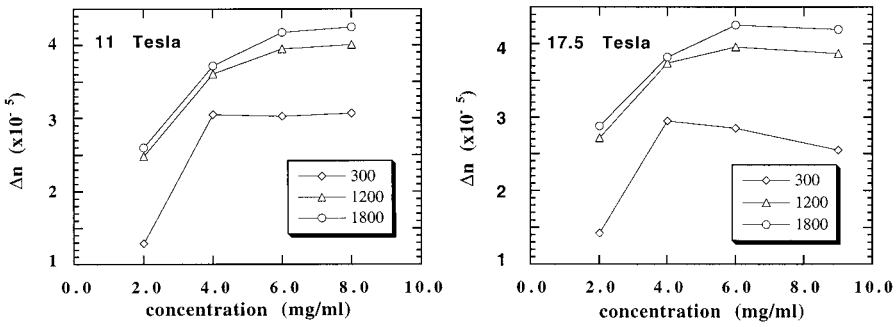

FIGURE 5 Birefringence as a function of microtubule concentration measured at three different times (300, 1200, and 1800 s) after the onset of the (temperature-induced) assembly for two magnetic field strengths. The curves are normalized for the variation in protein concentration, so that the birefringence value has a linear relation with the degree of alignment. The birefringence for the higher concentrations develops more slowly, but ultimately reaches a higher value for the higher protein concentrations (11 T *left*, 17.5 T *right*).

which, with the parameters used in this work, is ~28°C (Lee and Timasheff, 1977). It was therefore unexpected that the birefringence was influenced by the rate at which the temperature was raised from 4°C to 37°C. In Fig. 6 the development of the birefringence for different temperature ramp rates is shown.

In Fig. 6 the time scale is adapted for the different experiments such that the points where assembly starts coincide. It is clear that the slower temperature ramp rates result in a less birefringent sample. It should be remarked as well that when the temperature was raised in discrete steps of 5°C and equilibrated for 5 min after each step, no birefringence was observed, although the turbidity of the sample indicated that assembly had taken place. A point of interest is that with a rapid temperature increase, more polymerization nucleation sites will be created. With a constant tubulin concentration, this means that more microtubules will be formed, but that the average length of microtubules will be shorter. This is likely to have an effect on the dynamics of polymer entanglement. In a living "polymer system" like a treadmilling solution of microtubules, it is easy to see that possible misalignments will grow more easily out of the system than longer misaligned microtubules. A possible explanation for the absence of any alignment in the experiment where the temperature was raised in discrete steps could be that very few assembly nuclei were created, so that very long microtubules were created, which prevented alignment because of entanglements.

A parameter that influences the kinetics of the assembly process is the Mg concentration (Diaz et al., 1993). Increasing the Mg concentration speeds up the reaction. The birefringence results for assembly with different Mg concentrations are shown in Fig. 7.

Below the critical Mg concentration, no assembly takes place. The Mg concentration is also a parameter that determines the number of nucleation sites. With Mg concentrations of 11 mM and above, an excess of nucleation sites is formed and the birefringence shows an overshoot. Before the system can come to an equilibrium average length, some disassembly has to take place to allow other microtubules to grow at the expense of others. However, the short microtubules experience a smaller alignment force, and entanglement has probably taken place before the system reaches the equilibrium average length, and consequently the birefringence remains below the optimum.

In all dynamic experiments it was found that the conditions that favored the formation of a large number of nu-

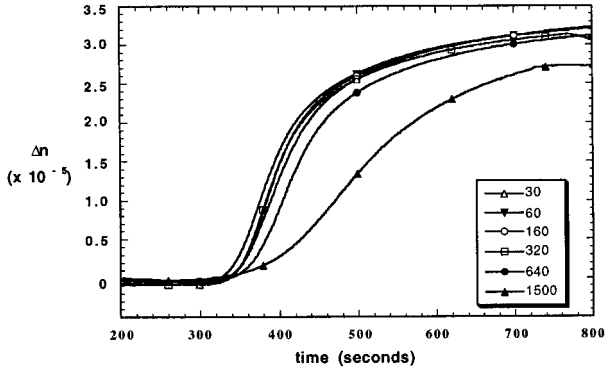

FIGURE 6 Development of the birefringence for samples that were heated with different rates from 4°C to 37°C. The fastest rates give a higher degree of alignment, whereas the slowest assembled samples systematically exhibit a weaker birefringence. For times exceeding 2 h, no increase in the birefringence was observed, although it was verified that assembly had taken place.

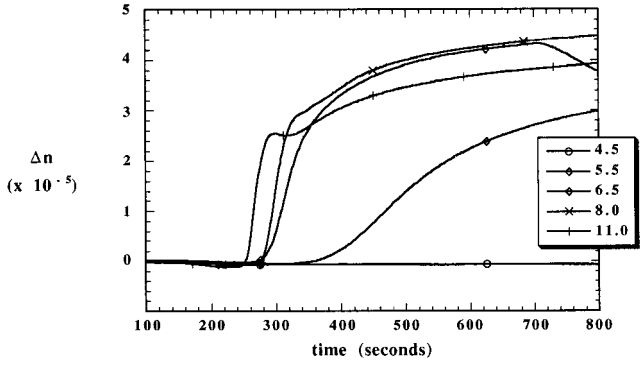

FIGURE 7 Birefringence for samples assembled by using the same temperature ramp rate but with different Mg^{2+} concentrations. Below the critical threshold no assembly takes place. A too high concentration creates a very large number of nucleation centers, leading to very short microtubule polymers. This is an out-of-equilibrium state that will only change after a portion of the macromolecules have donated material to other, larger microtubules. The shorter length also leads to a smaller diamagnetic anisotropy, which will lead to less alignment and hence a larger probability of forming an entangled, less aligned network.

cleation sites (high dimer concentration, high Mg concentration, rapid temperature ramp rate) generated the optimum alignment conditions for alignment, although the formation of too many nucleation sites was detrimental (Mg concentration $\geq$ 11 mM). This indicates that entanglement must play an important role. If a large number of short polymers are formed before entanglement becomes a major effect, the optimum alignment is reached. This is probably independent of the final average length when equilibrium is reached.

Fiber diffraction experiments

A representative example of a low-resolution fiber diffraction pattern is shown in Fig. 8. This pattern is obtained in ~1 h (protein concentration 4.2 mg/ml), which is sufficient to obtain reliable intensities from the stronger features on the equator of the diffraction pattern. The equator and first layer line can be distinguished. If the structure is assumed to be predominantly a 13 protofilament microtubule, the first three peaks on the equator of the fiber diffraction pattern can be indexed as being subsidiary maxima from a J_0 Bessel function (Mandelkow et al., 1977). The fourth strong peak is the J_{13} Bessel function maximum, which has its origin in the electron density fluctuations on the microtubule wall caused by the grooves between the protofilaments. Further details of the fiber diffraction pattern are beyond the scope of this paper and can be found in Amos and Klug (1974) and Beese et al. (1987).

An often ignored problem in x-ray fiber diffraction on biological systems are effects due to radiation damage. Based on the assumption that one 8-keV photon damages ~10 dimers (Nave, 1995), it can be calculated that an x-ray dose of 5.7×10^{12} photons/mm^3 will damage ~10% of the dimers (Bras, 1995). This is an x-ray dose that translates into a 4-min exposure to the x-ray beam on both stations 2.1 and 8.2, where these experiments have been performed. This is in good agreement with our empirical findings. Radiation damage is observed as a loss of orientation and a decrease in diffraction peak intensities.

In Fig. 9 the relation is given between the strength of the magnetic field and the degree of alignment as derived from fiber diffraction experiments on samples assembled inside a constant magnetic field and subsequently taken out of the magnetic field and placed on the synchrotron radiation beamline, for a constant protein concentration. As expected, the alignment improves with the strength of the field. Unfortunately, we are not able to obtain data from samples aligned in fields in excess of 11 T, because of the limited field strength available at the synchrotron radiation laboratory. These results are in qualitative agreement with the birefringence results.

The degree of alignment is determined by performing a radial integration over strong peaks on the equator of the

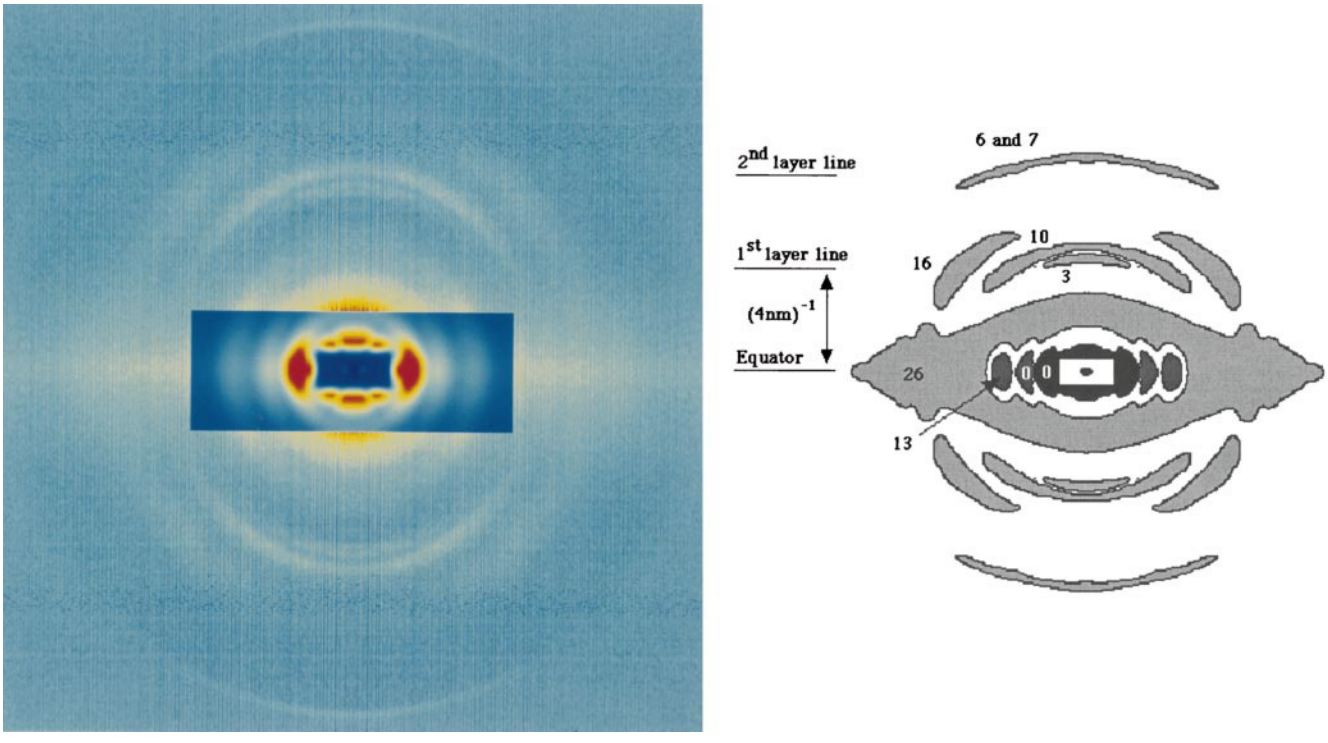

FIGURE 8 Low-resolution x-ray fiber diffraction pattern of an oriented solution of hydrated microtubules. Data shown are the average of data collected from six individual samples that were each exposed to the x-ray beam at a number of spots to avoid radiation damage. Total data collection time was 4 h. The contribution of the buffer solution to the diffraction pattern has been subtracted. The right-hand panel is a stylized trace indicating the main diffraction features. The rectangular box in the center represents an area with a higher threshold value (100×).

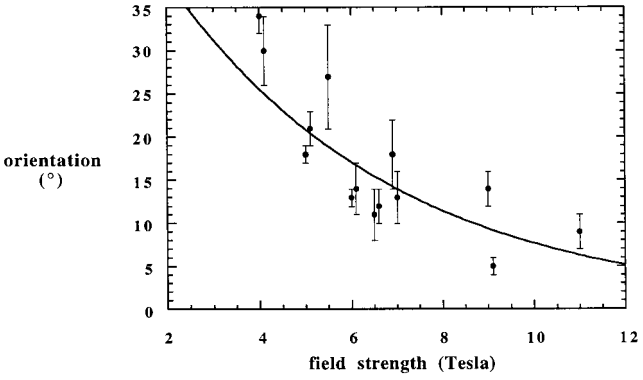

FIGURE 9 Degree of orientation for microtubules assembled inside a constant magnetic field as a function of magnetic field strength. After assembly, the samples were taken out of the magnetic field and placed in the fiber diffraction equipment. The protein concentration was 4.0 mg/ml. The points at 4 and 5.5 T were obtained in a single experimental session, and it cannot be ruled out that there is a systematic error in the protein concentration that will influence the degree of alignment. The other data points were also taken in a single experimental session.

diffraction pattern. The full width at half-maximum in the intensity distribution is defined to be the degree of orientation. This represents the angle with which the microtubule axes in a sample are distributed around the average orientation axis. It was found that the average orientation axis was parallel to the magnetic field direction. This is in agreement with the findings of Vassilev et al. (1982), who have studied the effects of magnetic and electric fields on the alignment of single microtubules, although these authors claim that they have successfully aligned microtubules in fields of 0.02 T, two orders of magnitude lower than used here and far below the values calculated in Eq. 5.

An exponential fit can be made to the data. However, at lower field strengths the results are less reliable, because of the fact that in samples assembled outside the field, a small degree of spontaneous orientation can sometimes be observed. This can possibly interfere with the magnetically induced alignment. For low degrees of orientation, ψ (radians) can be approximately expressed as a function of the square of the magnetic field (Bras, 1995):

$$\psi = \frac{p_{x,y} - p_z}{p_z} = -\frac{N\Delta\chi B^2}{2kT\mu_0} = -\frac{\Delta\chi B^2}{2kT\mu_0} \qquad (8)$$

in which $p_{x,y}$ is the probability that a molecule is aligned along the x and y axes, p_z is the probability that the molecule is aligned along the z axis (i.e., the magnetic field direction), N is the number of dimers in a microtubule, $\Delta\chi$ the diamagnetic susceptibility of a dimer, and B is the strength of the magnetic field. The magnitude of $\Delta\chi$ can be estimated from the ratio ψ/B^2, which was determined to be $(2.6 \pm 0.9) \times 10^{-3}$, leading to a value for $\Delta\chi = (2.6 \pm 0.9) \times 10^{-29}$ (note that $2kT\mu_0 = 1.04 \times 10^{-26}$). This is somewhat lower than the value of 10.1×10^{-29}, which was theoretically estimated for the component relevant for the alignment. However, a variation in the average number of dimers in a single microtubule or in the number of peptide bonds in α-helices parallel with the dimer axis or the presence of aromatic amino acids can easily influence these values. It should also be kept in mind that Eq. 8 is only an approximation of low degrees of alignment.

Discrepancies between the birefringence results and the fiber diffraction data can be observed when the orientation of the microtubules as function of the concentration is studied. In Fig. 10 the alignment is shown as a function of protein concentration for two different field strengths.

It can be seen that a higher protein concentration exhibits a lower orientation. Because the experimental protocol was the same in both the birefringence and diffraction experiments and the small decay in the birefringence, after the field is magnetic field is switched off, leaves the relative magnitudes of the birefringence intact, the cause for this discrepancy has to be the interaction between the x-rays and the microtubules. With a higher protein concentration the absolute number of absorbed photons, and consequently the absolute amount radiation damage, will increase. The disruptive effects on the orientation will be more severe for the higher protein concentrations. For a constant protein concentration, this effect obviously cannot be observed, which explains the agreement between the birefringence and diffraction results when the relation between magnetic field strength and orientation is studied.

The solid lines in Fig. 10 represent a least-squares fit to the data points. When the curves are extrapolated to a concentration of 0 mg/ml, they both converge to a value of $9° \pm 1°$.

Interestingly, diffraction patterns of samples that were rapidly assembled showed a high degree of alignment (~9°) that was independent of the protein concentration, but a loss of orientation became visible within 2 min. When viewed between crossed polarizers, it was clear that the whole sample had broken up into many domains that were tilted with respect to each other, even though the irradiation was localized in a single spot and the radiation-damaged mate-

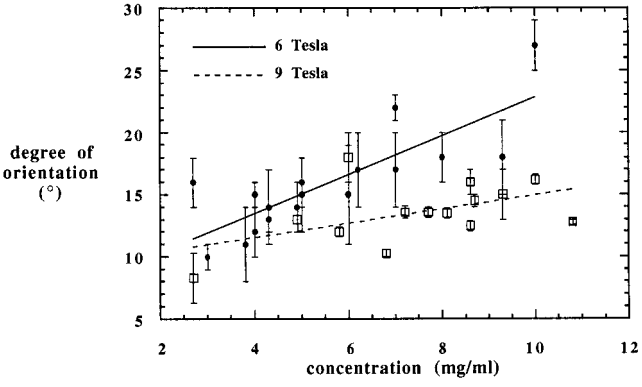

FIGURE 10 Degree of orientation as a function of the protein concentration for two magnetic field strengths. The straight lines represent a linear-squares fit to the data points and converge to a value of ~9°. This can tentatively be seen as the maximum degree of alignment achievable with this method.

rial was not transported through the cell. The breaking up into domains could not be initiated by either mechanical perturbations or localized heating (over a 1-mm^2 point) of the sample cell. From diffraction patterns it could be established that the domains had an orientation of 45° with respect to each other. Thus it can be concluded that the microtubules are in a metastable configuration when the orientation becomes very high. When parts of the sample become radiation-damaged, the tension in the system is locally released, causing severe orientational disruptions throughout the cell by a domino effect. We have not been able to establish whether structural changes occur when the microtubules are forced into a highly concentrated and oriented state. However, a degree of mechanical deformation has to be assumed for the system to be able to generate the forces that cause the alignment. This cannot be entirely explained by surface charges, because if this were the case it would not be possible to form a metastable equilibrium state.

The observation that the degree of alignment when extrapolated to 0 mg/ml concentration is the same as the degree of alignment observed for rapidly aligned samples, independent of the protein concentration, tentatively leads to the conclusion that ~9° is the highest degree of alignment that can be obtained with the magnetic alignment technique. The degree of alignment achieved by centrifuging the samples for extended periods (Mandelkow et al., 1977) is estimated to be ~4°, which is more favorable for fiber diffraction experiments. However, the lack of intramolecular interferences in the diffraction pattern and the certainty that we are studying hydrated microtubules indicate that the magnetic alignment method is appropriate for sample alignment in x-ray fiber diffraction.

To assess the quality of the x-ray diffraction patterns obtained with the magnetic alignment method, a comparison was made of the low-resolution equatorial data with previously published x-ray fiber diffraction and solution scattering data. The diffraction pattern was corrected for the angular spread, using the procedures outlined by Fraser et al. (1976). The programs LSQUINT and FTOREC (R. C. Denny, unpublished data) were used for this procedure. A low-resolution equatorial diffraction trace is shown in Fig. 11. The peaks indicated by $J_{0,n}$ are the first three maxima of the $|J_0|^2$ Bessel function, which is, to a first approximation, the Fourier transform of the microtubule cylinder. The peak indicated by J_{13} is the first maximum of the Bessel functions, which is generated by the grooves on the microtubule surface between the protofilaments. This Bessel function has zero intensity below the first maximum. It should be noted that the nomenclature J_{13} is used to be able to make comparisons with earlier work. Strictly speaking, we are dealing with a mixture of microtubules with different numbers of protofilaments, which all give rise to Bessel functions of order $|J_n|^2$, in which n is the protofilament number. However, with the biochemical conditions used in this work, the predominant number of protofilaments is 13. For details about the fiber diffraction pattern of microtubules, the reader is referred to Amos and Klug (1974) or to the more general work of Vainshtein (1966).

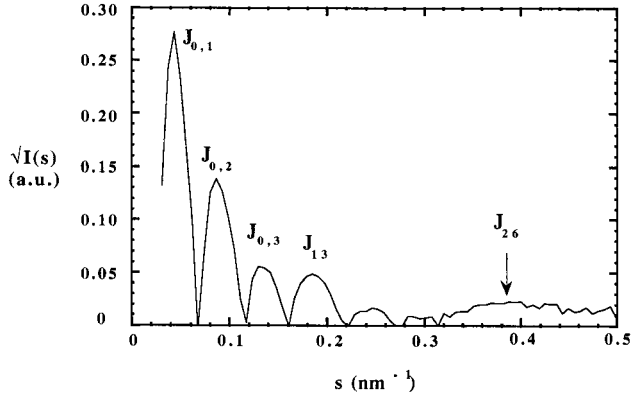

FIGURE 11 Equatorial intensity trace obtained from the fiber diffraction pattern. The original fiber diffraction pattern was corrected for angular spread by using the LSQUINT program. See text for details. The indications of the peaks are based on the work of Beese et al. (1987).

TABLE 1 Microtubule x-ray fiber diffraction equatorial peak parameters

		$J_{0,1}$	min	$J_{0,2}$	min	$J_{0,3}$	min	"J_{13}"
Oriented solution scattering (this work)	s nm^{-1}	0.043 ± 0.0005	0.07	0.088 ± 0.0005	0.12	0.134 ± 0.0005	0.0165	0.188 ± 0.0005
	i (a.u.)	100		25.26 ± 0.13		3.91 ± 0.13		3.13 ± 0.13
Fiber diffraction (Wais-Steider)	s	0.05	0.09	0.09	0.13	0.14	—	0.185
	i	100		34		5		5
Fiber diffraction (Beese)	s	0.045	0.07	0.095	0.12	0.135	0.164	0.185
	i	100		34		5		4
Solution scattering (Andreu)	s	0.050	0.08	0.095	0.12	0.135	0.164	0.185
	i	100		24		3		7

Values for s are in nm^{-1}; intensity values are given in arbitrary units in which the $J_{0,1}$ peak has been assigned a value 100. The columns marked min indicate the position of the minima between the peaks. The fiber diffraction data comparisons and terminology are taken from Wais-Steider et al. (1987) and Beese et al. (1987). The latter is a more thoroughly analyzed pattern, obtained following the alignment method first used by Mandelkow et al. (1977). For comparison, parameters obtained by solution scattering (Andreu et al., 1992) are also given. These experiments were performed in a protein concentration regime similar to that of the experiments described in this paper. The values obtained for the J_{13} peak will be distorted because of the fact that higher order subsidiary J_0 maxima will be superimposed on this peak. By limiting the comparison to $s = 0.185$ nm^{-1}, we avoid discrepancies that might rise from the overlap between the first layer line and the higher s-value data of the equator. This is impossible to avoid in the solution scattering experiments.

In Table 1 a comparison is made between the fiber diffraction results from Beese et al. (1987), Wais-Steider et al. (1987), and the solution scattering results from Andreu et al. (1992). It is clear that the intensity trace of the magnetically aligned microtubules closely follows the solution scattering results from Andreu et al. (1992). The $|J_0|^2$ Bessel function peaks decay more rapidly than in the fiber diffraction results from Beese et al. (1987) and Wais-Steider et al. (1987). The samples that were used by Beese et al. (1987) had been centrifuged for 24 h and after that rehydrated. However, the degree of rehydration is possibly not complete. There is good agreement between these two data sets. Because the data from Wais-Steider et al. (1987) were obtained from hydrated axons, it is clear that dehydration alone cannot be the cause of the differences. Therefore the most likely cause for the discrepancies between data obtained in this work and the solution scattering data from Andreu et al. (1992), as compared to Wais-Steider et al. (1987) and Beese et al. (1987), probably has to be sought in the absence of diffraction intensity, because of the crystallographic packing of the microtubules. A more detailed analysis of the fiber diffraction pattern, including a discussion of the details of layer line intensities and a comparison with the diffraction pattern of microtubules assembled in the presence of taxol, will be given in a forthcoming paper (Bras et al., manuscript in preparation).

CONCLUSIONS

It has been shown that pure microtubules are indeed highly birefringent. The strength of the birefringence signal is slightly lower than that found in dehydrated mitotic spindles, which consist to a large extent of microtubules. However, keeping in mind the different conditions, the similarity in magnitude obtained with these two techniques is remarkable.

The susceptibility of microtubules to magnetic fields has unequivocally been shown. The Cotton-Mouton constant of the tubulin dimer is below the detection limit of our equipment, but the diamagnetic anisotropy of assembled microtubules is sufficiently high that a high degree of alignment can be induced in microtubule solutions with a concentration of up to 10 mg/ml. This allows us to obtain aligned hydrated microtubule samples free from possible mechanical deformations suitable for quantitative fiber diffraction experiments on hydrated microtubules. An important parameter in obtaining the maximum degree of alignment is the assembly speed of the microtubules in the magnetic field. Rapid assembly produces highly aligned samples. However, great care has to be taken in performing x-ray fiber diffraction experiments, because the samples with the highest degree of orientation appear to be very sensitive to distortions of the alignment due to radiation damage.

As for the source of the diamagnetism, no conclusions can be drawn on the basis of the experiments reported here. The calculations based on a simplified model that ignores the possible contribution of aromatic amino acids are reasonably in line with the experimental results and can be used as an order-of-magnitude assessment for further investigations only.

The degree of orientation that can be achieved is sufficient to extract relevant parameters for the low-resolution structure of microtubules. Fiber diffraction patterns have been obtained for which the low-resolution diffraction data were in better agreement with solution scattering data than those obtained with alternative ways of sample preparation.

To obtain reliable high-resolution x-ray fiber diffraction patterns, it would be desirable for the samples to be contained in the high magnetic field while the x-ray diffraction data are collected, because there is nearly full alignment in these circumstances. The features that are now seen as diffraction arcs would contract into smaller arcs, which would influence the signal/background ratio in the diffraction patterns considerably. With present superconducting magnet technology, it is possible to build a split coil magnet for such experiments.

We acknowledge the technical assistance of Colin Clarke, Dave Bouch, Paul Hindley, and Jim Sheldon at Daresbury Laboratory. Our colleagues Colin Nave, Jim Torbet, Rudolf Oldenbourger, John Baldwin, and Chantal Dumortier have given valuable assistance and advice. Ruben Lebermann and Steve Cusack are thanked for making available the facilities at the EMBL outstation in Grenoble. The Netherlands Organisation for Scientific Research (NWO) and CCLRC Daresbury Laboratory made generous amounts of beam time available at the SRS. The European Community Large Scale Facility program gave us access to the Grenoble High Magnetic Field Laboratory.

HK received financial support from the European Community.

REFERENCES

Amos, L. 1979. *In* Microtubules. R. Hyams, editor. Academic Press, San Diego. Chapter: Structure of Microtubules.

Amos, L. A., and A. Klug. 1974. Arrangement of subunits in flagellar microtubules *J. Cell. Sci.* 14:523–549.

Andreu, J. M., J. Bordas, J. F. Diaz, J. Garcia de Ancos, R. Gil, F. J. Medrano, E. Nogales, E. Pantos, and E. Towns-Andrews. 1992. Low resolution structure of microtubules in solution. *J. Mol. Biol.* 226: 169–184.

Andreu, J. M., J. Garcia de Ancos, D. Starling, J. L. Hodgkinson, and J. Bordas. 1989. A synchrotron X-ray scattering characterisation of purified tubulin and of its expansion induced by mild detergent binding. *Biochemistry.* 28:4036–4040.

Andreu, J. M., M. J. Gorbunoff, J. C. Lee, and S. N. Timasheff. 1984. Interaction of tubulin with functional colchicine analogues: an equilibrium study. *Biochemistry.* 23:1742–1752.

Beese, L., G. Stubbs, and C. Cohen. 1987. Microtubule structure at 18 Å resolution. *J. Mol. Biol.* 194:257–264.

Bernal, J. D., and I. Fankuchen. 1941. X-ray and crystallographic studies of plant virus preparations. *J. Gen. Physiol.* 25:111–146.

Bordas, J., E-M. Mandelkow, and E. Mandelkow. 1983. Stages of tubulin assembly and disassembly studied by time resolved synchrotron x-ray scattering. *J. Mol. Biol.* 164:89–135.

Boulin, C., R. Kempf, M. H. J. Koch, and S. M. McLaughlin. 1986. Data appraisal, evaluation and display for synchrotron radiation experiments: hardware and software. *Nucl. Instr. Methods.* A249:399–407.

Bras, W. 1995. An x-ray fiber diffraction study of magnetically aligned microtubules in solution. Ph.D. Thesis. John Moores University, Liverpool, England.

Bras, W., G. E. Derbyshire, A. J. Ryan, G. R. Mant, P. Manning, R. E. Cameron, and W. Mormann. 1993. Simultaneous time resolved x-ray scattering experiments in the small and wide angle region. *J. Physique IV*. 3:447–450.

Diaz, J. F., J. M. Andreu, G. Diakum, E. Towns-Andrews, and J. Bordas. 1996. Structural intermediates in the assembly of taxol induced microtubules and GDP-tubulin double rings: time resolved x-ray scattering. *Biophys. J.* 70:2408–2420.

Diaz, J. F., M. Menendez, and J. M. Andreu. 1993. Thermodynamics of ligand induced assembly of tubulin. *Biochemistry.* 32:10067–10077.

Edwards, S. F. 1966. The theory of polymer solutions at intermediate concentration. *Proc. Phys. Soc.* 88:266–280.

Fraser, R. D. B., T. P. Macrae, A. Miller, and R. J. Rowlands. 1976. Digital processing of fiber diffraction patterns. *J. Appl. Crystallogr.* 9:81–94.

Gittes, F., B. Mickey, J. Nettleton, and J. Howard. 1993. Flexural rigidity of microtubules and actin filaments measured from thermal fluctuations in shape. *J. Cell. Biol.* 120:923–934.

Hayter, J. B., R. Pynn, S. Charles, A. T. Skjeltorp, J. Trewhella, G. Stubbs, and P. Timmins. 1989. Ordered macromolecular structures in ferrofluid mixtures. *Phys. Rev. Lett.* 62:1667–1670.

Himes, R. H., P. R. Burton, and J. M. Gaito. 1977. Dimethylsulfoxide-induced self assembly of tubulin lacking associated proteins. *J. Biol. Chem.* 252:222–6228.

Hirokawa, N., S-I. Hisanaga, and Y. Shiomura. 1988. MAP2 is a component of crossbridges and neurofilaments in neural cytoskeleton. *J. Neurosci.* 8:2769–2779.

Hitt, A. L., A. R. Cross, and R. C. Williams. 1990. Microtubule solutions display nematic liquid crystalline structure. *J. Biol. Chem.* 265: 1639–1647.

Hyams R., editor. 1979. Microtubules. Academic Press, San Diego.

Koch, M. H. J., Z. Sayers, P. Sicre, and D. Svergun. 1995. A synchrotron radiation electric field X-ray solution scattering study of DNA at very low ionic strengths. *Macromolecules.* 28:4904–4907.

Lee, J. C., D. Corfman, R. P. Frigon, and S. N. Timasheff. 1978. Conformation study of calf brain tubulin. *Arch. Biochem. Biophys.* 185:4–14.

Lee, J. C., R. P. Frigon, and S. N. Timasheff. 1973. The chemical characterisation of calf brain microtubule protein subunits. *J. Biol. Chem.* 248:7272–7262.

Lee, J. C., and S. N. Timasheff. 1977. In vitro reconstitution of calf brain microtubules: effect of solution variables. *Biochemistry.* 16:1754–1764.

Lewis, R. A., J. S. Worgan, N. S. Fore, I. L. Sumner, F. d'Annunzio, A. Berry, B. Parker, K. Roberts, and G. R. Mant. 1989. The application of multiwire proportional counters to experiments utilising synchrotron radiation. *SPIE Proc.* 1159:205–216.

Little, M., and T. Seehaus. 1988. Comparative analysis of tubuline sequences. *Comp. Biochem. Physiol.* 90:655–670.

Mandelkow, E. 1986. X-ray diffraction of cytoskeletal fibers. *Methods Enzymol.* 134:657–667.

Mandelkow, E., J. Thomas, and C. Cohen. 1977. Microtubule structure at low resolution by x-ray diffraction. *Proc. Natl. Acad. Sci. USA.* 74: 3370–3374.

Maret, G., and K. Dransfeld. 1985. Biomolecules and polymers in high steady magnetic fields. *Top. Appl. Phys.* 57:143–204.

Mills, N. J. 1972. Optical properties. *In* Polymer Science. A. D. Jenkins, editor. North-Holland, Amsterdam.

Murphy, D. B., and G. G. Borisy. 1975. Association of high molecular weight proteins with microtubules and their role in microtubule assembly in vitro. *Proc. Natl. Acad. Sci. USA.* 72:2696–2700.

Nave, C. 1995. Radiation damage in protein crystallography. *Radiat. Phys. Chem.* 45:483–490.

Nave, C., R. Brown, A. Fowler, J. Ladner, D. Marvin, S. Provencher, A. Tsugita, J. Armstrong, and R. Perham. 1981. Pf1 filamentous bacterial virus: x-ray diffraction analysis of two heavy atom derivatives. *J. Mol. Biol.* 149:675–707.

Nave, C., A. G. Fowler, S. Malsey, D. A. Marvin, H. Siegrist, and E. J. Wachtel. 1979. Macromolecular structural transitions in Pf1 filamentous bacterial virus. *Nature.* 281:232–234.

Nogales de la Morena, E. 1992. The assembly of microtubule and drug induced tubulin polymers: an x-ray diffraction and cryo-electron microscopy study. Ph.D. thesis. Keele University, Keele, England.

Nogales, E., S. G. Wolf, I. A. Khan, R. F. Luduena, and K. H. Downing. 1995. Structure of tubulin at 6.5 Å and location of the taxol binding site. *Nature.* 375:424–427.

Onsager, L. 1949. The effect of shape on the interactions of colloidal particles. *Ann. N.Y. Acad. Sci.* 51:627–659.

Pauling, L. 1979. Diamagnetic anisotropy of the peptide group. *Proc. Natl. Acad. Sci. USA.* 76:2293–2294.

Pirollet, F., D. Job, R. Margolis, and J. Garel. 1987. An oscillatory mode for microtubule assembly. *EMBO J.* 6:3247–3252.

Popp, D., V. V. Lednev, and W. Jahn. 1987. Methods of preparing well oriented sols of f-actin containing filaments suitable for fiber diffraction. *J. Mol. Biol.* 197:679–684.

Rothwell, S. W., W. A. Grassev, and D. B. Murphy. 1986. End-to-end annealing of microtubules in vitro. *J. Cell. Biol.* 102:619–624.

Samulski, E. T., and A. V. Tobolsky. 1971. Distorted alpha helix for poly(gamma-benzyl L-glutamate) in the nematic solid state. *Biopolymers.* 10:1013–1019.

Sato, H., G. W. Ellis, and S. Inoué. 1975. Microtubular origin of mitotic spindle form birefringence. *J. Cell Biol.* 67:501–517.

Sosnick, T., S. Charles, G. Stubbs, P. Yau, E. M. Bradbury, P. Timmins, and J. Trewhella. 1991. Orienting rigid and flexible biological assemblies in ferrofluids for small angle neutron scattering. *Biophys. J.* 60: 1178–1189.

Torbet, J. 1987. Using magnetic orientation to study structure and assembly. *Trends Biochem. Sci.* 12:327–330.

Torbet, J. 1995. Laboratoire d'Elaboration par Procédés Magnetiques, Grenoble. Unpublished results.

Torbet, J., and M. J. Dickens. 1984. Orientation of skeletal muscle actin in strong magnetic fields. *FEBS Lett.* 173:403–406.

Torbet, J., J.-M. Freyssinet, and G. Hudry-Clergeon. 1981. Oriented fibrin gels formed by polymerization in strong magnetic fields. *Nature.* 289: 91–93.

Torbet, J., and G. Maret. 1979. Fibres of highly oriented Pf1 bacteriophage produced in a strong magnetic field. *J. Mol. Biol.* 134:843–845.

Torbet, J., and G. Maret. 1981. High-field magnetic birefringence study of the structure of rodlike phages Pf1 and fd in solution. *Biopolymers.* 20:2657–2669.

Torbet, J., and M. Ronzière. 1984. Magnetic alignment of collagen during self-assembly. *Biochem. J.* 219:1057–1059.

Towns-Andrews, E., A. Berry, J. Bordas, G. R. Mant, P. K. Murray, K. Roberts, I. S. Sumner, J. S. Worgan, and R. Lewis. 1989. Time-resolved x-ray diffraction station: x-ray optics, detectors and data acquisition. *Rev. Sci. Instrum.* 60:2346–2349.

Vainshtein, B. K. 1966. Diffraction of X-Rays by Chain Molecules. Elsevier, New York.

Vassilev, P. M., R. T. Dronzine, M. P. Vassileva, and G. A. Georgiev. 1982. Parallel arrays of microtubules formed in electric and magnetic fields. *Biosci. Rep.* 2:1025–1029.

Venier, P., A. C. Maggs, M. F. Carlier, and D. Pantaloni. 1994. Analysis of microtubule rigidity using hydrodynamic flow and thermal fluctutations. *J. Biol. Chem.* 269:13353–13360.

Ventilla, M., C. R. Cantor, and M. Shelanski. 1972. A circular dichroism study of microtubule protein. *Biochemistry.* 11:1554–1561.

Vroege, G. J., and H. N. W. Lekkerkerker. 1992. Phase transitions in lyotropic colloidal and polymer liquid crystals. *Rep. Prog. Phys.* 55: 1241–1309.

Wais-Steider, C., N. S. White, D. S. Gilbert, and P. M. Eagles. 1987. X-ray diffraction patterns from microtubules and neurofilaments in axoplasm. *J. Mol. Biol.* 197:205–218.

Weisemberg, R. C., G. G. Borisy, and E. Tailor. 1968. The colchicine binding protein of mammalian brain and its relationship to microtubules. *Biochemistry.* 7:4466–4479.

Wicke, G. 1985. High molecular weigth microtubule associated proteins. *Trends Biochem Sci.* 10:67–70.

Worcester, D. L. 1978. Structural origins of diamagnetic anisotropy in proteins. *Proc. Natl. Acad. Sci. USA.* 75:5475–5477.